Res Chem Intermed (2011) 37:11–17
DOI 10.1007/s11164-010-0228-0

Rapid consolidation of nanostructured Ti from mechanically activated Ti and TiH_2 by pulsed-current activated sintering, and the mechanical properties of the product

Na-Ri Kim · In-Yoong Ko · Sung-Wook Cho · Wonbaek Kim · In-Jin Shon

Received: 1 July 2010 / Accepted: 24 October 2010 / Published online: 2 December 2010

Abstract Dense nanostructured Ti was sintered from mechanically activated Ti and TiH_2 powders by pulsed-current activated heating under a pressure of 80 Mpa. TiH_2 powder was decomposed to Ti during sintering. The hardness of the Ti increased, and the average grain size of the Ti decreased, with increasing milling time.

Keywords Sintering · Nanomaterials · Hardness · Ti

Introduction

Use of titanium in dentistry and medicine has become well established because of the combination of excellent biocompatibility, low density of 4.54 g cm^{-3}, and corrosion resistance compared with the more conventional stainless steels [1, 2]. Commercially pure titanium is chemically inert and biologically more compatible than Ti-6Al-4V, but coarse-grained Ti has low wear and abrasion resistance because of its low hardness [3]. To improve its mechanical properties, the approach commonly utilized has been to make nanostructured materials.

N.-R. Kim · I.-Y. Ko · I.-J. Shon
Division of Advanced Materials Engineering, the Research Center of Advanced Materials Development, Chonbuk National University, Jeonju, Jeonbuk 561-756, Republic of Korea

S.-W. Cho · W. Kim
Minerals and Materials Processing Division, Korea Institute of Geoscience, Mining and Materials Resources, Daejeon, Republic of Korea

I.-J. Shon (✉)
Department of Hydrogen and Fuel Cells Engineering, Specialized Graduate School, Chonbuk National University, Jeonju, Jeonbuk 561-756, Republic of Korea
e-mail: ijshon@chonbuk.ac.kr

Because nanomaterials undoubtedly have high strength, high hardness, excellent ductility and toughness, much attention has been paid to their application [4, 5]. Nanocrystalline powders have recent been developed by the thermochemical and thermomechanical process called the "spray conversion process" (SCP), by co-precipitation, and by high-energy milling [6–8]. However, the grain size in sintered materials is much larger than that in pre-sintered powders because of fast grain growth during conventional sintering. Therefore, controlling grain growth during sintering is one of the keys to commercial success of nanostructured materials. In this regard, the pulsed-current activated sintering method which can make dense materials within 2 min, has been shown to be effective in achieving this objective [9, 10].

The purpose of this study was to produce dense nanocrystalline Ti within 2 min from mechanically activated Ti and TiH_2 powders, by using the pulsed-current activated sintering method, and to evaluate its hardness and grain size.

Experimental procedure

Powders of 99.5% Ti (400 mesh; Sezong) and 99% TiH_2 (400 mesh; Sezong) were used as a starting materials. The Ti and TiH_2 powders were first milled at 250 rpm for 5 h in a high-energy Pulverisette-5 planetary ball mill. Tungsten carbide balls (8.5 mm in diameter) were used in a sealed cylindrical stainless steel vial under argon atmosphere. The ball-to-powder weight ratio was 30:1.

After milling, the mixed powders were placed in a graphite die (outside diameter 45 mm; inside diameter 20 mm; height 40 mm) and then introduced into the pulsed-current (on time 20 μs, off time 10 μs) activated sintering system (Eltek, South Korea; described elsewhere [9, 10]). The four major stages in the sintering were as follows. The system was evacuated (stage 1) and a uniaxial pressure of 80 MPa was applied (stage 2). A pulsed current was then activated and maintained until densification was attained as indicated by a linear gauge measuring the shrinkage of the sample (stage 3). Temperature was measured by use of a pyrometer focused on the surface of the graphite die. At the end of the process, the sample was cooled to room temperature (stage 4).

The relative densities of the sintered sample were measured by the Archimedes method. Microstructural information was obtained from product samples which were polished and etched using a solution of HF (2 ml), HNO_3 (5 ml), and H_2O (100 ml) for 1 min at room temperature. Compositional and micro structural analyses of the products were performed by X-ray diffraction (XRD) and scanning electron microscopy (SEM) with energy dispersive X-ray analysis (EDAX). Vickers hardness was measured by performing indentations at a load of 50 kg and with a dwell time of 15 s on the sintered samples.

The grain sizes of Ti and TiH_2 were calculated by use of C. Suryanarayana and M. Grant Norton's formula [11],

$$B_{\mathrm{r}}\left(B_{\mathrm{crystalline}} + B_{\mathrm{strain}}\right)\cos\theta = \mathrm{k}\lambda/\,\mathrm{L} + \eta\sin\theta \qquad (1)$$

where B_r is the full width at half-maximum (FWHM) of the diffraction peak after instrument correction; $B_{crystalline}$ and B_{strain} are FWHM caused by small grain size and internal stress, respectively, k is a constant (with a value of 0.9), λ is the wavelength of the X-ray radiation, L and η are grain size and internal strain, respectively, and θ is the Bragg angle. B and B_r follow Cauchy's form with the relationship: $B = B_r + B_s$, where B and B_s are the FWHM of the broadened Bragg peaks and the standard sample's Bragg peaks, respectively.

Results and discussion

XRD patterns of the raw materials and the milled powder are shown in Fig. 1. The full width at half-maximum of the diffraction peak for the milled powder is wider than that for the raw powder because of strain and refinement of grain size. The average grain sizes of Ti and TiH_2 milled for 5 h, calculated by use of C. Suryanarayana and M. Grant Norton's formula [11], were approximately 31 nm and 12 nm, respectively.

The changes in shrinkage displacement and temperature of the surface of the graphite die with heating time during the processing of Ti and TiH_2 system are shown Fig. 2. As the pulsed current was applied, the sample showed thermal expansion. The shrinkage displacement of TiH_2 abruptly increased at approximately 700 °C. However, the shrinkage displacement of Ti gradually increased to 1000 °C as soon as the pulsed current was applied. It is considered that the difference of sintering behavior of Ti and TiH_2 is because TiH_2 is decomposed to Ti and H_2 during the sintering. It is reported that the decomposition temperature of TiH_2 is approximately 430 °C [12].

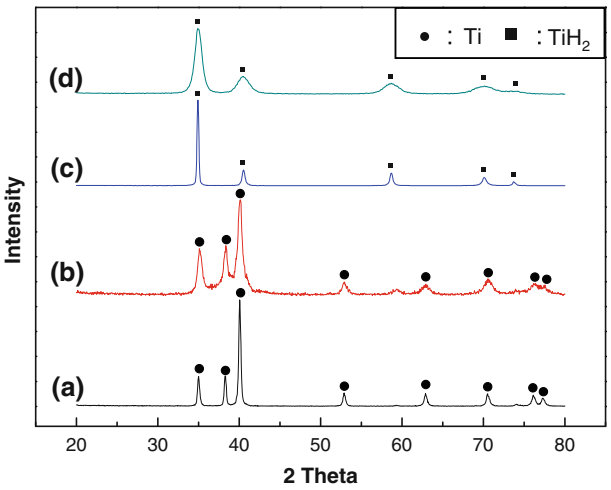

Fig. 1 XRD patterns of the Ti and TiH_2 powder milled for different times: Ti (*a*) 0 h, (*b*) 5 h, TiH_2 (*c*) 0 h, (*d*) 5 h

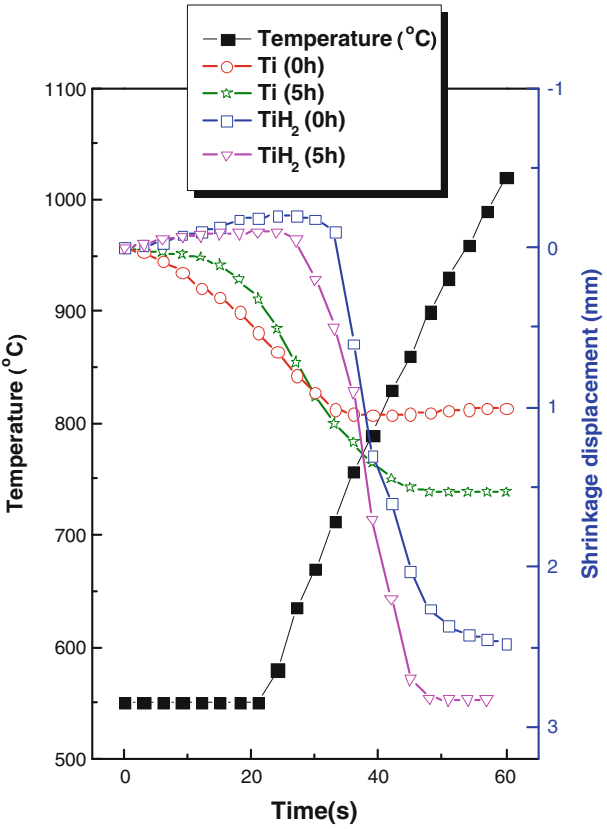

Fig. 2 Variations of temperature and shrinkage displacement with heating time during pulsed-current activated sintering of Ti and TiH_2 powder with milling time: Ti (*a*) 0 h, (*b*) 5 h, TiH_2 (*c*) 0 h, (*d*) 5 h

X-ray diffraction results, shown in Fig. 3 show peaks pertaining to the Ti only. The full width at half-maximum of the diffraction peak in Ti sintered from milled powder is wider than that of Ti sintered from unmilled powder, because of the refinement of grain size. The average grain sizes of Ti sintered from Ti and TiH_2 powders milled for 5 h [11] were 42 nm and 80 nm, respectively. The grain size of sintered Ti is not much greater than that of the starting powder milled for 5 h. The reasons for rapid sintering without great grain growth are as follows. The role of the inductive current in sintering has been the focus of several attempts aimed at providing an explanation of the observed enhancement of the sintering process and the improved characteristics of the products. The role played by the current has been variously interpreted, the effect being explained in terms of the fast heating rate because of Joule heating, the presence of a plasma in the pores separating the powder particles, and the intrinsic contribution of the current to mass transport [13–15]

Figure 4 shows SEM (scanning electron microscope) images of Ti and TiH_2 samples heated to 1020 °C. The grain size of Ti decreased with increasing milling

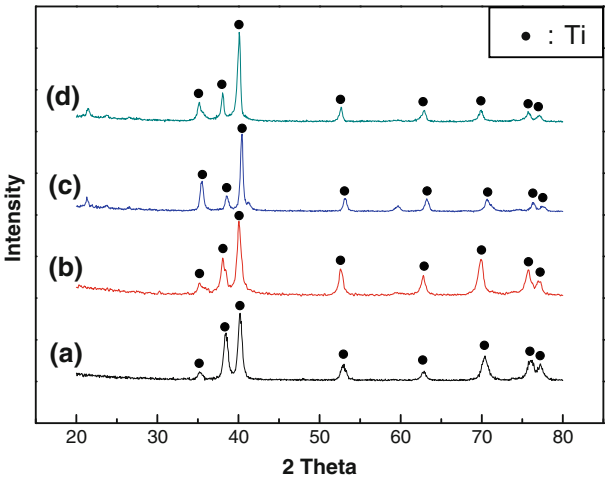

Fig. 3 XRD patterns of the Ti sintered from Ti and TiH_2 powder milled for various time: Ti (*a*) 0 h, (*b*) 5 h, TiH_2 (*c*) 0 h, (*d*) 5 h

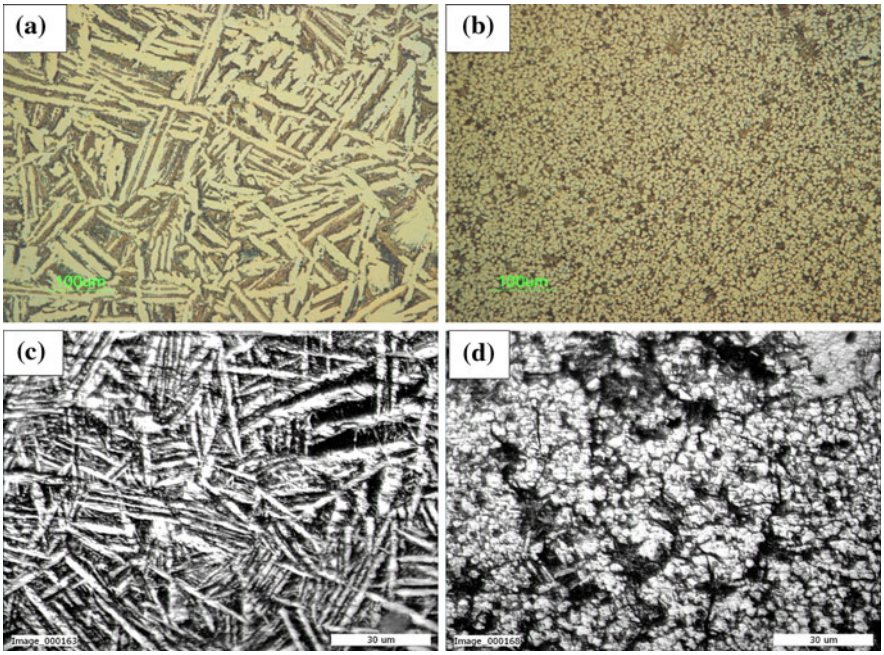

Fig. 4 SEM images of Ti sintered from Ti and TiH_2 powder milled for various times: Ti **a** 0 h, **b** 5 h, TiH_2 **c** 0 h, **d** 5 h

time. FE-SEM images of Ti sintered from the powders milled for 5 h are shown in Fig. 5. It is apparent from the figure that Ti consisted of nanoparticles.

Vickers hardness measurements were made on polished sections of the Ti using a 50 kg_f load and 15 s dwell time. Calculated hardness values of Ti sintered from Ti

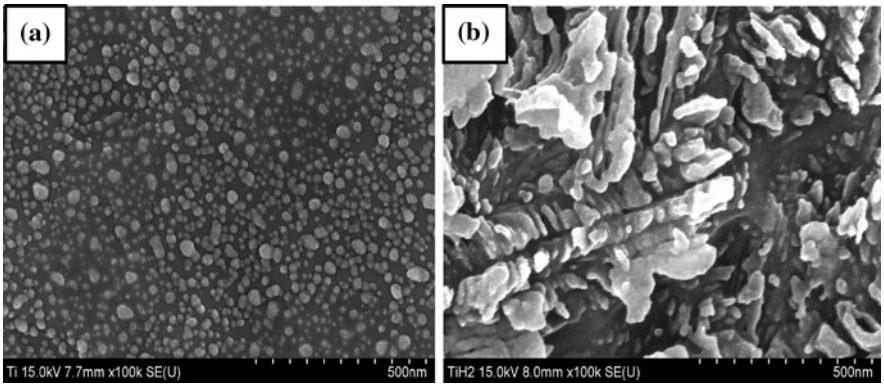

Fig. 5 FE-SEM images of Ti sintered from powders milled for 5 h: **a** Ti, **b** TiH_2

powder milled for 0 and 5 h were 350 and 510 kg/mm^2, respectively. Calculated hardness values of Ti sintered from TiH_2 powder milled for 0 and 5 h were 340 and 575 kg/mm^2, respectively. These values are averages from five measurements. The hardness of Ti sintered from milled Ti and TiH_2 is much greater because of refinement of grain.

Use of TiH_2 instead of Ti does not lead to any reduction in mechanical properties. Given the advantage of the lower cost of TiH_2, the results are significant for potential applications.

Conclusions

Using the pulsed-current activated sintering method, densification of nanostructured Ti was accomplished from mechanically activated powders of Ti and TiH_2. Complete densification can be achieved within 1 min. The average grain sizes of Ti sintered from Ti and TiH_2 powders milled for 5 h by pulsed-current activated sintering were approximately 42 and 80 nm, respectively. The average hardness of Ti sintered from milled Ti and TiH_2 were 510 and 575 kg/mm^2, respectively. Use of TiH_2 instead of Ti does not result in any reduction in mechanical properties. Given the advantage of the lower cost of TiH_2, the results are significant for potential applications.

Acknowledgment This study was supported by a grant from basic research project of Korea Institute of Geoscience and Mineral Resources.

References

1. M. Long, H.J. Rack, Biomaterials **19**, 1621–1639 (1998)
2. X.Y. Liu, P.K. Chu, C.X. Ding, Mater. Sci. Eng. **47**, 49–121 (2004)
3. S. Berger, R. Porat, R. Rosen, Prog. Mater. Sci. **42**, 311–320 (1997)
4. L. Fu, L.H. Cao, Y.S. Fan, Scripta Mater. **44**, 1061–1068 (2001)

5. Z. Fang, J.W. Eason, Int. J. Refractory Met. Hard Mater **13**, 297–303 (1995)
6. A.I.Y. Tok, l.h. Luo, F.Y.C. Boey, Mater. Sci. Eng. **383**, 229–234 (2004)
7. I.J. Shon, D.K. Kim, K.T. Lee, K.S. Nam, Met. Mater. Int. **14**, 593–598 (2008)
8. H.C. Kim, I.J. Shon, J.K. Yoon, J.M. Doh, Met. Mater. Int **12**, 141–146 (2006)
9. H.C. Kim, I.J. Shon, I.K. Jeong, I.Y. Ko, Met. Mater. Int **12**, 393–398 (2006)
10. C. Suryanarayana, M. Grant Norton, X-ray diffraction a practical approach (Plenum Press, New York, 1998), pp. 212–213
11. Y.W. Gu, M.S. Yong, B.Y. Tay, C.S. Lim, Mater. Sci. Eng. **29**, 1515–1520 (2009)
12. Z. Shen, M. Johnsson, Z. Zhao, M. Nygren, J. Am. Ceram. Soc. **85**, 1921–1927 (2002)
13. J.E. Garay, U. Anselmi-Tamburini, Z.A. Munir, S.C. Glade, P. Asoka-Kumar, Appl. Phys. Lett. **85**, 573–578 (2004)
14. J.R. Friedman, J.E. Garay, U. Anselmi-Tamburini, Z.A. Munir, Intermetallics **12**, 589–597 (2004)
15. J.E. Garay, J.E. Garay, U. Anselmi-Tamburini, Z.A. Munir, Acta Mater. **51**, 4487–4495 (2003)